Int. J. Heat Mass Transfer. Vol. 9, pp. 1125–1144. Pergamon Press 1966. Printed in Great Britain

CONDENSATION HEAT TRANSFER IN THE PRESENCE OF NONCONDENSABLES, INTERFACIAL RESISTANCE, SUPERHEATING, VARIABLE PROPERTIES, AND DIFFUSION

W. J. MINKOWYCZ† and E. M. SPARROW

Heat Transfer Laboratory, Department of Mechanical Engineering, University of Minnesota, Minneapolis, Minnesota

(*Received* 6 *January* 1966 *and in revised form* 21 *February* 1966)

Abstract—A wide-ranging analytical investigation of laminar film condensation is presented. The situation under study is an isothermal vertical plate with steam as the condensing vapor and air as the noncondensable gas. In addition to the noncondensable gas, the analytical model includes interfacial resistance, superheating, free convection due to both temperature and concentration gradients, mass diffusion and thermal diffusion, and variable properties in both the liquid and the gas-vapor regions. Heat-transfer results are obtained for a wide range of parameters including bulk concentration of the noncondensable gas, system pressure level, wall-to-bulk temperature difference, and degree of superheating. It is demonstrated that small bulk concentrations of the noncondensable gas can have a decisive effect on the heat-transfer rate. For instance, for a bulk mass fraction of air equal to 0·5 per cent, reductions in heat transfer of 50 per cent or more are sustained. The influence of the noncondensable gas is accentuated at lower pressure levels. It is shown that the aforementioned reductions in heat transfer are due entirely to the diffusional resistance of the gas–vapor boundary layer. The interfacial resistance is shown to be a second order effect. A similar finding applies to thermal diffusion and diffusion thermo. The effect of superheating, which is very small in the case of a pure vapor, becomes much more significant in the presence of a noncondensable gas. A reference temperature rule is deduced for extending the Nusselt model to variable-property conditions.

NOMENCLATURE

C, c, constants, equations (16) and (2b);
c_p, specific heat, constant pressure;
D, binary diffusion coefficient;
F, f, dimensionless stream functions;
g, acceleration of gravity;
h_{fg}, latent heat of condensation;
j, diffusive mass flux, equation (9);
k, thermal conductivity;
M, molecular weight;
$M, \dot{m}$, interface mass flux;
p, total pressure;
p_v, vapor pressure;
Pr, Prandtl number, $c_p\mu/k$;
q, wall heat flux;
q^*, generalized heat flux, equation (11);
R, gas constant;
Sc, Schmidt number, ν/D;
T, temperature;
$T_{sat,\infty}$, bulk saturation temperature;
T_∞, bulk temperature;
T_w, wall temperature;
T_δ, interface temperature;
T^*, reference temperature, equation (37);
u, v, velocity components;
W, mass fraction;
x, y, coordinates.

Greek symbols

α, thermal diffusion factor;
δ, condensate film thickness;
H, η, similarity variables;
Θ, θ, dimensionless temperature;
μ, absolute velocity;
ν, kinematic viscosity;

† Present address: Department of Energy Engineering, University of Illinois at Chicago Circle, Chicago, Illinois 60680.

ρ, density;
σ, condensation coefficient;
Φ, φ, property ratios;
Ψ, ψ, stream functions.

Subscripts

g, noncondensable gas;
Nu, from the Nusselt model;
v, vapor;
w, at the wall;
δ, at the interface;
∞, in the bulk.

INTRODUCTION

FILM CONDENSATION on isothermal vertical surfaces has been a subject of active analytical study since the pioneering analysis of Nusselt [1]. In the intervening years, the various simplifying assumptions embodied in that first investigation have been relaxed so that, with certain reservations, the solution of Nusselt's problem may now be regarded as complete. An extensive bibliographical survey of contributions to this problem area has been prepared by Wilhelm [2]. The physical situation studied by Nusselt and in various succeeding investigations is, perhaps, the simplest of all problems in laminar film condensation: namely, a pure, quiescent, saturated vapor condensing on an isothermal vertical plate.

A class of condensation problems of much greater complexity is encountered when consideration is given to vapors which contain noncondensable gases. In such situations, concentration and temperature gradients are set up in the vapor–gas mixture (temperature gradients will occur if the vapor component is at its saturation state). Correspondingly, buoyancy forces, owing to both concentration and temperature differences, are created. Furthermore, the thermodynamic and transport properties of the vapor–gas mixture may experience large variations. A full description of the transport processes in the mixture requires that the conservation equations for mass, energy, momentum, and species be written in their variable property forms. The dynamic interaction of the aforementioned transports in the vapor–gas mixture produces a temperature at the liquid–vapor interface that is lower than the saturation temperature of the bulk vapor.

Another physical mechanism of potential importance is the so-called interfacial resistance. This phenomenon may occur for both pure and impure vapors, but its analytical evaluation is much more formidable in the latter case. In brief, the interfacial resistance results from the fact that the net condensation of vapor at the interface is actually the difference between the simultaneous processes of evaporation and condensation. The kinetic theory of gases shows that an unbalance between these two processes must be accompanied by a temperature jump at the interface, whence the additional thermal resistance.

Another departure from the classical Nusselt model is encountered when the vapor is superheated. Although the effect of superheating on the condensation heat transfer rate is expected to be small in the case of a pure vapor, it may well be appreciable when factors such as noncondensable gases and interfacial resistance act to reduce the rate of condensation.

Whenever there are concentration and temperature gradients in a gas mixture such as occur during the condensation of an impure vapor, the processes of thermal diffusion and diffusion thermo come into play. The first of these is a transport of mass owing to a temperature gradient, while the second is an energy transport owing to a concentration gradient. In certain technically-important problems, for example, mass-transfer cooling, these processes have a significant influence on the surface heat transfer. Their effect on the condensation of impure vapors is, as yet, unexplored.

This investigation is concerned with the influence of all of the aforementioned processes and conditions on laminar condensation on an isothermal vertical plate. The extent to which these factors affect the condensation heat transfer is systematically studied as a function of the

system pressure level. In view of its technical importance, steam was selected as the condensing vapor for the present investigation, with air as the noncondensable gas.

Inasmuch as such a wide range of effects is to be dealt with, it appears advantageous to list the main lines of the present research.

(1) Pure vapor: (a) interfacial resistance; (b) superheating.
(2) Noncondensable gas: (a) with and without interfacial resistance; (b) with and without superheating.
(3) Superheated vapor: (a) with and without interfacial resistance; (b) with and without noncondensable gas.
(4) Interfacial resistance: (a) saturated and superheated pure vapor; (b) saturated and superheated vapor with a noncondensable gas.
(5) Thermal diffusion and diffusion thermo: (a) saturated and superheated vapor with a noncondensable gas.
(6) Variable property effects in the condensed liquid layer.

In all of the aforementioned cases in which there are temperature (and concentration) gradients within the vapor (and the vapor–gas mixture), variable fluid property variations were fully taken into account, as was the buoyancy force which creates a free convection motion. As noted in the foregoing item (6), variable property effects in the condensate layer were also included in the analysis. A reference temperature rule was evolved which serves to extend the Nusselt model.

Limited aspects of the just-described research program are treated in the literature by approximate models. The effect of superheating a pure vapor has been studied by Stender [3] and by Sparrow and Eckert [4], respectively with a one-dimensional model and a boundary-layer model. In both cases, free convection, variable properties, and interfacial resistance were omitted from the analysis. Silver [5, 6] employed Stender's model for analyzing the effect of interfacial resistance on the condensation of a pure, superheated vapor. In the case of a pure, saturated vapor, Sukhatme and Rohsenow [7] computed the effect of the interfacial resistance by local application of the results of the Nusselt analysis.

Various semi-empirical analyses and computation methods have been proposed for predicting the condensation heat transfer in the presence of noncondensable gases ([8, 9] or standard heat transfer textbooks). Very recently on the basis of the conservation laws alone, Sparrow and Lin [10] analyzed the condensation of saturated steam–air mixtures. However, variable fluid properties, temperature-induced buoyancy, and interfacial resistance were not accounted for in that analysis, nor were the processes of thermal diffusion and diffusion thermo, which occur naturally in a vapor–gas mixture.

The variation of the fluid properties within the condensate film are generally neglected in analytical studies of condensation heat transfer. However, in the actual application of the heat transfer results from such a model, it is common to evaluate the liquid viscosity at a reference temperature equal to the wall value plus one-quarter of the temperature difference across the film [11]. The choice of such a reference temperature appears not yet to have been substantiated by detailed numerical computations.

Consideration of the just-discussed directly-pertinent literature suggests the need for a broad-ranging, in-depth study such as is reported here.

In the presentation that follows, it is convenient to subdivide the analysis into two portions, one dealing with condensation in the absence of interfacial resistance and the second dealing with condensation in the presence of interfacial resistance. This subdivision is natural inasmuch as the former situation yields similarity solutions of the appropriate boundary layer equations, while the latter does not.

ANALYSIS OF CONDENSATION WITHOUT INTERFACIAL RESISTANCE

Consideration is given to an isothermal

vertical plate situated adjacent to a large body of otherwise quiescent vapor. The vapor may either be at its saturation state or be superheated. Furthermore, the vapor may contain arbitrary amounts of a noncondensable gas. When the plate temperature is maintained at a value below the saturation temperature, condensation will occur. It is assumed that the condensate forms a smooth film† which flows downward along the plate under the influence of gravity. It is natural to regard the condensate film as a boundary layer.

The condensation process activates the transport of mass, momentum, energy, and species in the vapor–gas mixture adjacent to the condensate film. The region in which these transports occur may also be regarded as a boundary layer. Thus, there are a pair of co-existing, interacting boundary layers, one in the liquid and one in the vapor–gas mixture. It is convenient to formulate the governing equations separately for the two boundary layers, and then to couple them by applying conditions of compatibility at the interface.

The coordinates that are employed in the analysis are as follows: x measures distances (vertically downward) along the plate, with $x = 0$ coinciding with the leading edge; y measures distances normal to the plate. The corresponding velocity components are u and v. The thickness of the condensate layer is defined as $y = \delta(x)$.

Liquid boundary layer

The transport processes in the liquid boundary layer are governed by the laws of mass, momentum, and energy conservation. There is no diffi-

layer equations. However, it has been demonstrated [12] that the inertia terms and the energy convection terms have a negligible effect on heat transfer for the range of parameter values‡ appropriate to steam. In view of this, one may employ a simplified set of boundary layer equations as follows

$$\frac{\partial}{\partial x}(\rho u) + \frac{\partial}{\partial y}(\rho v) = 0 \tag{1a}$$

$$\rho g + \frac{\partial}{\partial y}\left(\mu \frac{\partial u}{\partial y}\right) = 0 \tag{1b}$$

$$\frac{\partial}{\partial y}\left(k \frac{\partial T}{\partial y}\right) = 0. \tag{1c}$$

The continuity equation is identically satisfied by introducing a stream function ψ, which, in turn, may be reduced to a similarity stream function f that depends only on a single independent coordinate η. The appropriate definitions are

$$u = \frac{1}{\varphi_\rho}\frac{\partial \psi}{\partial y}, \qquad v = -\frac{1}{\varphi_\rho}\frac{\partial \psi}{\partial x},$$

$$\psi = 4\nu_w c x^{\frac{3}{4}} f(\eta) \tag{2a}$$

$$\eta = c\frac{y}{x^{\frac{1}{4}}}, \qquad c = \left(\frac{g}{4\nu_w^2}\right)^{\frac{1}{4}}, \qquad \theta = \frac{T}{T_\infty} \tag{2b}$$

in which a dimensionless temperature variable θ has also been introduced. Upon carrying out the foregoing transformation of variables, the conservation laws are reduced to a pair of ordinary differential equations

$$\left[\varphi_\mu\left(\frac{f'}{\varphi_\rho}\right)'\right]' + \varphi_\rho = 0, \qquad \left(\varphi_k \theta'\right)' = 0 \tag{3}$$

where the primes denote derivatives with respect to η and

$$\varphi_\rho = \frac{\rho}{\rho_w}, \qquad \varphi_\mu = \frac{\mu}{\mu_w}, \qquad \varphi_k = \frac{k}{k_w} \tag{4}$$

the φ are temperature-dependent functions.

The boundary conditions appropriate to equation (3) will be described later. For future reference, it is convenient to derive expressions for the streamwise velocity u_δ at the liquid–vapor interface and for the mass flow per unit area $\dot{m}$ crossing the interface. The former follows directly from equations (2) as

$$u_\delta = 4\nu_w c^2 x^{\frac{1}{2}}\left(\frac{f'}{\varphi_\rho}\right)_{\eta_\delta}. \tag{5}$$

† The effect of ripples is to increase the heat transfer; this is discussed in [24].

‡ i.e. values of $c_p(T_{sat} - T_w)/h_{fg}Pr$.

The quantity $\dot{m}$ is related to the velocity components u and v as follows

$$\dot{m}\,dx = (\rho u\,d\delta - \rho v\,dx)_\delta. \tag{6}$$

Upon introducing the transformed variables, this becomes

$$\dot{m} = \left(\frac{3c\mu_w}{x^{\frac{1}{4}}}\right) f(\eta_\delta). \tag{7}$$

Vapor–gas boundary layer

There is a considerably wider range of transport processes taking place in the vapor–gas boundary layer than in the just-discussed liquid boundary layer. The additional processes include diffusional mass and heat transfers and free convection.

In a two-component gas mixture, it is convenient to represent the local concentrations of the components in terms of their mass fractions W. These are defined as

$$W_g = \rho_g/\rho, \qquad W_v = \rho_v/\rho \tag{8a}$$

where ρ is the local density of the mixture and ρ_g and ρ_v are, respectively, the local densities of the gas and the vapor. Since $\rho = \rho_g + \rho_v$, it follows that

$$W_g + W_v = 1. \tag{8b}$$

In view of equation (8b), W_g and W_v are not independent, and one of them may be eliminated from the problem. In this analysis, it has been decided to retain W_g and to drop its subscript; therefore, in what follows, $W_g \equiv W$.

Owing to concentration and temperature gradients, a diffusive mass flux j (per unit time and area) is induced. For instance, the diffusive mass flux of the gas, denoted by j_g, is

$$j_g = -\rho D\left[\frac{\partial W}{\partial y} + \frac{\alpha W(1-W)}{T}\frac{\partial T}{\partial y}\right] \tag{9}$$

in which D is the binary diffusion coefficient and α is the thermal diffusion factor.† The first term within the brackets is the well-known mass diffusion, while the second term represents thermal diffusion. A similar expression can be written for the diffusive flow of the vapor, j_v. Upon noting that the value of α appearing in the j_g equation is the negative of that appearing in the j_v equation, it is seen that

$$j_v = -j_g. \tag{10}$$

The generalized heat flux q^* per unit time and area in a binary mixture includes both convective and diffusive contributions and is given by

$$q^* = -k\frac{\partial T}{\partial y} + \alpha RT\frac{M^2}{M_g M_v} j_g \tag{11}$$

in which R and M respectively denote the local gas constant and molecular weight of the mixture, while M_g and M_v are the molecular weights of the components. The first term in equation (11) is immediately recognized as the conventional Fourier conduction, while the second term represents diffusion thermo.

In a binary mixture, mass must be conserved for each of the components. This requirement may be satisfied by writing a diffusion equation for each of the species, or alternatively a continuity equation for the mixture and a diffusion equation for one of the species. The latter approach is somewhat more convenient and will be employed here.

Consideration may now be given to the boundary-layer equations for the vapor–gas region. The equations of continuity, diffusion, momentum, and energy may be respectively written as

$$\frac{\partial}{\partial x}(\rho u) + \frac{\partial}{\partial y}(\rho v) = 0 \tag{12}$$

$$\rho\left(u\frac{\partial W}{\partial x} + v\frac{\partial W}{\partial y}\right) = -\frac{\partial j_g}{\partial y} \tag{13}$$

$$\rho\left(u\frac{\partial u}{\partial x} + v\frac{\partial u}{\partial y}\right) = g(\rho - \rho_\infty) + \frac{\partial}{\partial y}\left(\mu\frac{\partial u}{\partial y}\right) \tag{14}$$

† This is not to be confused with the thermal diffusivity $k/\rho c_p$.

$$\rho c_p\left(u\frac{\partial T}{\partial x}+v\frac{\partial T}{\partial y}\right)+(c_{p_g}-c_{p_v})j_g\frac{\partial T}{\partial y}=-\frac{\partial q^*}{\partial y}. \quad (15)$$

The generalized diffusive mass flux and heat flux, j_g and q^* respectively, are given by equations (9) and (11). The quantity, $g(\rho-\rho_\infty)$, appearing in equation (14) is the buoyancy force, which induces a free-convection motion. This term is to be retained as written; that is, the usual linear density–temperature approximation will not be made. Another somewhat novel term is the quantity $(c_{pg}-c_{pv})j_g(\partial T/\partial y)$ in equation (15). This represents a net enthalpy flux owing to the diffusion currents j_g and $j_v\,(=-j_g)$.

The foregoing conservation equations can be reduced to a set of ordinary differential equations by employing a similarity transformation as follows

$$\Psi=4\nu_\infty Cx^{\frac{3}{4}}F(H),\qquad H=\frac{C}{x^{\frac{1}{4}}}\int_\delta^y\frac{dy}{\Phi_\mu},$$

$$\Theta=\frac{T}{T_\infty},\qquad C=\left(\frac{g}{4\nu_\infty^2}\right)^{\frac{1}{4}} \quad (16)$$

in which Ψ is a stream function that satisfies

$$u=\frac{1}{\Phi_\rho}\frac{\partial\Psi}{\partial y},\qquad v=-\frac{1}{\Phi_\rho}\frac{\partial\Psi}{\partial x}. \quad (17)$$

The end result of the transformation is

$$\left(\frac{W'}{Sc}\right)'+3Sc\,F\left(\frac{W'}{Sc}\right)=-\Gamma' \quad (18)$$

$$\left(\frac{F'}{\Phi_\mu\Phi_\rho}\right)''+3F\left(\frac{F'}{\Phi_\mu\Phi_\rho}\right)'-\left[\frac{2F'^2}{\Phi_\mu\Phi_\rho}+\Phi_\mu(1-\Phi_\rho)\right]=0 \quad (19)$$

$$\left(\frac{\Phi_k}{\Phi_\mu}\Theta'\right)'+Pr_\infty\left(3\Phi_c F+\Phi_{c_{gv}}\frac{W'}{Sc}\right)\Theta'=-Pr_\infty(\Lambda'+\Phi_{c_{gv}}\Gamma\Theta') \quad (20)$$

in which

$$\Gamma=\frac{\alpha}{Sc}W(1-W)\frac{\Theta'}{\Theta}, \quad (21a)$$

$$\Lambda=\frac{\alpha R\Theta}{c_{p_\infty}}\frac{M^2}{M_gM_v}\left(\frac{W'}{Sc}+\Gamma\right) \quad (21b)$$

and

$$\Phi_\rho=\frac{\rho}{\rho_\infty},\qquad \Phi_k=\frac{k}{k_\infty},\qquad \Phi_\mu=\frac{\mu}{\mu_\infty},$$

$$\Phi_c=\frac{c_p}{c_{p_\infty}} \quad (21c)$$

$$\Phi_{c_{gv}}=\frac{c_{p_g}-c_{p_v}}{c_{p_\infty}} \quad (21d)$$

The quantities Sc and Pr respectively represent the local mixture Schmidt and Prandtl numbers. All of the thermodynamic and transport properties appearing in the foregoing equations are functions of the local temperature and concentration of the mixture. The primes denote differentiation with respect to H.

Upon reconsideration of equations (18) and (20), it is seen that the non-zero right-hand sides are due exclusively to the thermal diffusion/diffusion thermo effects. When these phenomena are suppressed, as in a majority of the cases studied here, then the corresponding right-hand sides are equated to zero. Even with this simplification, equations (18) through (20) remain a highly-coupled, highly non-linear, seventh-order mathematical system. The solution of this system and its coupling to the equations of the liquid layer are discussed later.

In order to facilitate the aforementioned coupling, it is useful to derive expressions for the velocity u_δ and the mass flux $\dot{M}$ of the vapor–gas mixture that crosses the interface per unit time and area. From equations (16) and (17), there follows directly

$$u_\delta=4\nu_\infty C^2x^{\frac{1}{2}}\left(\frac{F'}{\Phi_\mu\Phi_\rho}\right)_{H=0}. \quad (22)$$

In deriving an expression for the mass flux, cognizance must be taken of both diffusive and convective components and of the contributions of both species. To this end, one writes

$$\dot{M} = \dot{M}_g + \dot{M}_v \tag{23}$$

and

$$\dot{M}_k = \left[\left(\rho_k u \frac{\mathrm{d}\delta}{\mathrm{d}x} - \rho_k v\right) + j_k\right], \qquad k = g, v \tag{24}$$

where the quantity in parentheses is the convective mass flow and j is the diffusive mass flow. Upon combining the foregoing equations and noting that $\rho_g + \rho_v = \rho$, $j_g + j_v = 0$, there is obtained

$$\dot{M} = \left(\rho u \frac{\mathrm{d}\delta}{\mathrm{d}x} - \rho v\right)_\delta. \tag{25}$$

Then, after transformation in accordance with equations (16) and (17) this becomes

$$\dot{M} = \left(\frac{3C\mu_\infty}{x^{\frac{1}{4}}}\right) F(0). \tag{26}$$

Attention will now be directed to the boundary conditions and to the conditions of continuity and constraint at the interface.

Boundary and interface conditions; governing parameters

To complete the statement of the problem, it remains to specify conditions at the plate surface, at the liquid–vapor interface, and in the bulk of the vapor–gas mixture.

At the plate surface ($y = 0$), the temperature T_w is prescribed and the velocity components u and v are zero. In terms of the transformed variables, these become

$$f = f' = 0, \qquad \theta = \theta_w \tag{27}$$

at $\eta = 0$.

At the interface, there are both continuity and constraint conditions. In general, the interfacial shear, the streamwise velocity, the mass flux, the temperature, and the energy flux must be continuous at the interface. With respect to the interfacial shear, it has been demonstrated [12] that the neglect of the continuity requirement has a completely negligible effect on the heat-transfer results for the range of parameters appropriate to condensing steam. Furthermore, owing to the lower condensation rates associated with the presence of noncondensable gases, the application of this finding in the present analysis is fully justified. It is thus sufficient to impose the Nusselt condition of negligible shear at the edge of the liquid layer, that is, $\mu\, \partial u/\partial y = 0$ at $y = \delta$ ($\eta = \eta_\delta$), or

$$\left(\frac{f'}{\varphi_\rho}\right)' = 0. \tag{28}$$

The continuity of the streamwise velocity u_δ is implemented by equating expressions (5) and (22), which gives

$$(f'/\varphi_\rho)_{\eta_\delta} = (F'/\Phi_\mu \Phi_\rho)_0 \tag{29}$$

Similarly, the continuity of the mass flux is achieved by requiring that $\dot{m} = \dot{M}$ and using equations (7) and (26)

$$(\rho_w \mu_w / \rho_\infty \mu_\infty)^{\frac{1}{2}} f(\eta_\delta) = F(0). \tag{30}$$

Temperature continuity is imposed by writing

$$\theta(\eta_\delta) = \Theta(0). \tag{31}$$

In order to formulate the condition of energy-flux continuity, it is convenient to consider a control volume that envelopes the interface. An accounting of the various energy transports leads to

$$\left(k \frac{\partial T}{\partial y}\right)_{\text{liquid}} = \dot{M} h_{fg} - q^* \tag{32}$$

in which h_{fg} is the latent heat of condensation and q^* is the generalized heat flux as given by equation (11). In deriving equation (32), it has been assumed that the interface is impermeable to the noncondensable gas. Upon rephrasing equation (32) in terms of the variables of the

analysis, one finds

$$\left(\frac{\rho_w\mu_w}{\rho_\infty\mu_\infty}\right)^{\frac{1}{2}}\frac{c_{p_w}Pr_\infty}{c_{p_\infty}Pr_w}(\varphi_k\theta')_{\eta_\delta} = \frac{3Pr_\infty h_{fg}}{c_{p_\infty}T_\infty}F(0) + \left(\frac{\Phi_k}{\Phi_\mu}\Theta'\right)_0 + Pr_\infty\Lambda(0). \quad (33)$$

In addition to the foregoing continuity requirements, there are two conditions of constraint at the interface. The first is that the interface is impermeable to the noncondensable gas; that is $\dot{M}_g = 0$. Upon applying this condition to equation (24) and introducing the transformed variables, there is obtained

$$\left[3FW + \left(\frac{W'}{Sc} + \Gamma\right)\right]_0 = 0. \quad (34)$$

The second constraint is that the interface be a saturation state for the condensing vapor. In effect, this condition provides a connecting link between the interface temperature T_δ and the interface mass fraction W. This relationship may be illuminated as follows: For a given interface temperature T_δ, the corresponding vapor pressure p_v and vapor density ρ_v are uniquely determined from the saturation-state relationship (e.g. from the Steam Tables). Furthermore, if the total pressure p is specified, then the partial pressure p_g of the non-condensable gas follows from the Gibbs–Dalton Law as $p_g = p - p_v$. Thus, from a knowledge of p_g and T_δ, the density ρ_g is calculable (e.g. from the perfect gas law). Finally, the W corresponding to the given T_δ follows as $W = \rho_g/(\rho_g + \rho_v)$.

In the bulk of the vapor-gas mixture (i.e. $y \to \infty$), it is required that $u \to 0$, $T \to T_\infty$ and $W \to W_\infty$, or alternatively

$$F' = 0, \qquad W = W_\infty, \qquad \Theta = 1 \quad (35)$$

as $H \to \infty$.

Upon reconsideration of the governing equations, the boundary conditions, and the nature of the property variations, the following independent parameters emerge: T_w, T_∞, p, and W_∞. It was found more convenient to work with a somewhat different set of parameters. Let $T_{\text{sat},\infty}$ denote the *saturation* temperature of the vapor in the bulk.† With this, the working parameters were selected as follows: T_w, $T_{\text{sat},\infty}$ $(T_\infty - T_{\text{sat},\infty})$, W_∞. It may be verified that the total pressure p is readily derivable from these. The quantity $(T_\infty - T_{\text{sat},\infty})$ is a direct measure of the degree of superheating.

Thermodynamic and transport properties

A knowledge of the fluid properties is an essential prerequisite for the solution of the governing equations. Detailed information about the properties is available in Appendix A of the thesis [13] from which this paper is drawn. Only a brief outline is presented here.

The properties ρ, μ, k, and c_p of liquid water were taken from tabulations by Eckert and Drake [14] to which were fitted high-accuracy algebraic expressions. For the steam–air mixture, rules derived by Mason and Monchick [15] from the kinetic theory of transport properties were employed in the computation of μ, k, D, and α. Values of ρ and c_p were calculated by standard additive procedures.

The properties μ, k, and c_p of pure air and pure steam were taken from the NBS tables [16], except for c_p of steam, which is available in algebraic form in the Steam Tables [17]. Air was treated as a perfect gas, while equation (13) of [17] served as the equation of state for steam. The latent heat of condensation h_{fg} and the vapor pressure–temperature relationship at saturation were algebraically fitted according to values in the Steam Tables.

Generally speaking, the property calculations for the mixture were quite lengthy and complex, especially those for the transport properties. It is believed that the property values used in the analysis are the best presently available.

Solutions

Upon reviewing the governing equations, boundary conditions, continuity conditions,

† That is, corresponding to p_v in the bulk.

and constraints, it is evident that the task of obtaining solutions is particularly formidable. The fact that there are two co-existing variable-property boundary layers which are coupled by six conditions of continuity and constraint makes for difficulties well beyond those encounted in the typical boundary-layer problem. Naturally, it was necessary to employ numerical means to achieve solutions; but even with a computer such as the CDC 1604, the time requirement was measurable in tens of hours.

In carrying out the solutions, it was found convenient to work with integral equations rather than with differential equations, the former permitting the direct incorporation of some of the boundary and continuity conditions. The integral equations were solved by a special iterative process which is described in detail in [13], Chapter 3.

Heat transfer parameters; Nusselt-model reference temperature

The result of major interest is the heat transfer to the plate surface ($y = 0$). Upon applying Fourier's Law $q = (k\ \partial T/\partial y)_{y=0}$ in conjunction with the variables defined in equations (2), there follows

$$q = k_w(g/4xv_w^2)^{\frac{1}{4}}\ T_\infty\ \theta'(0). \tag{36}$$

The quantity $\theta'(0)$ is given by the numerical solution of the governing equations.

It was decided that a meaningful presentation of results would be achieved by comparing the heat transfer in the presence of noncondensables, superheating, interfacial resistance, etc., with that of the standard Nusselt model. In applying the Nusselt expression, it is necessary to specify the thermal driving force and the reference temperature for evaluating the thermodynamic and transport properties. For the former, it is reasonable to employ $(T_{sat,\infty} - T_w)$. A proper reference temperature was derived as part of this investigation.

To determine the reference temperature, numerical solutions of the governing equations (3) for the liquid layer were carried out for prescribed values of $T_\delta \equiv T_{sat,\infty}$ ranging from 671·7°R (212°F) to 539·7°R (80°F), that is, pressure levels ranging from approximately one atmosphere to 0·5 psi. For these runs, the temperature difference $(T_\delta - T_w)$ was varied from 2 degF to 45 degF. The variable-property heat-transfer results thus obtained were compared with those of the Nusselt constant-property analysis. It was found that virtual coincidence between the two sets of results could be achieved by evaluating all the properties† appearing in the Nusselt expression at the reference temperature T^* defined by

$$T^* = T_w + 0{\cdot}31\,(T_\delta - T_w). \tag{37}$$

With the specifications of the preceding paragraphs, the wall heat flux from the Nusselt model becomes

$$\frac{q_{Nu}x}{h_{fg}\mu^*} = \left[\frac{c_p^*(T_{sat,\infty} - T_w)}{h_{fg}Pr^*}\right]^{\frac{1}{4}}\left(\frac{gx^3}{4\nu^{*2}}\right)^{\frac{1}{4}}. \tag{38}$$

All of the heat transfer results presented in this paper are in the form of q/q_{Nu}. Inasmuch as both q and q_{Nu} are proportional to $x^{-\frac{1}{4}}$, this quantity cancels out of the ratio. In evaluating the reference temperature, T_δ is taken as $T_{sat,\infty}$.

ANALYSIS OF CONDENSATION WITH INTERFACIAL RESISTANCE

A widely-accepted model of the condensation process [2, 5–7, 18–21] states that the saturation temperature of the vapor adjacent to the surface of the condensate is different from the temperature of the liquid at that surface. This temperature jump is attributed to the simultaneous process of evaporation and condensation that take place at the surface. An expression characterizing the temperature jump was derived by Schrage [18] on the basis of simple kinetic

† Except h_{fg} which is evaluated at T_δ.

theory.† Schrage's expression has been reworked by Balekjian and Katz [19] into a more tractable, but somewhat approximate form as follows (see also [7])

$$\dot{m} = \left(\frac{\sigma}{2-\sigma}\right)\left(\frac{2}{\pi R_v^3}\right)^{\frac{1}{2}}\left[\frac{p_{v,\delta}h_{fg}}{T_{\delta,v}^{\frac{3}{2}}}(T_{\delta,v} - T_{\delta,L})\right]. \tag{39}$$

In this equation, σ is the condensation coefficient characterizing the fraction of the vapor molecules striking the liquid surface which actually condense; evidently, $0 \leqslant \sigma \leqslant 1$. $T_{\delta,v}$ is the saturation temperature of the vapor adjacent to the liquid surface ($p_{v,\delta}$ is the corresponding saturation pressure of the vapor) and $T_{\delta,L}$ is the temperature of the liquid surface.

For the special case in which $T_{\delta,v} \equiv T_{\text{sat},\infty}$ (pure, saturated vapor), it is possible to take account of the inter-facial resistance and still obtain an exact solution of the condensation problem. For purposes of comparison, a solution based on the *local-similarity* concept will also be derived for this case. When a non-condensable gas and/or superheating are involved, then the presence of the interfacial resistance precludes an exact solution and local similarity must be employed.

Pure saturated vapor

For this situation, it is only necessary to deal with the governing equations for the condensate layer. Inasmuch as a reference temperature rule, equation (37), has been established, property variations may be set aside and equations (1) may be written as

$$\frac{\partial u}{\partial x} + \frac{\partial v}{\partial y} = 0, \qquad \rho g + \mu\frac{\partial^2 u}{\partial y^2} = 0, \qquad \frac{\partial^2 T}{\partial y^2} = 0. \tag{40}$$

These are to be solved subject to the following boundary conditions, respectively at $y = 0$ and $y = \delta$

$$u = v = 0, \qquad T = T_w \tag{41a}$$

$$\frac{\partial u}{\partial y} = 0, \qquad \dot{m} = \Omega(T_{\delta,v} - T_{\delta,L}),$$

$$T_{\delta,v} = T_{\text{sat},\infty} \tag{41b}$$

where

$$\Omega = \left(\frac{\sigma}{2-\sigma}\right)\left(\frac{2}{\pi R_v^3}\right)^{\frac{1}{2}}\left(\frac{p_{v,\delta}h_{fg}}{T_{\delta,v}^{\frac{3}{2}}}\right). \tag{42}$$

Owing to the fact that $T_{\delta,v}$ is a prescribed constant, the quantity Ω is also a constant. The condensate temperature $T_{\delta,L}$ at $y = \delta$ is an unknown function of x.

The foregoing set of equations can be solved without approximation. The details will be omitted here, and only the essential results are outlined. The condensate layer thickness δ is given by the following quartic algebraic equation

$$\delta^4 + \left(\frac{4k}{3h_{fg}\Omega}\right)\delta^3 = \frac{4\nu^2}{g}\left[\frac{c_p(T_{\text{sat},\infty} - T_w)}{Pr\, h_{fg}}\right]x \tag{43}$$

where the second term on the left stems from the presence of the interfacial resistance. Once $\delta(x)$ has been determined from the foregoing, then the interfacial temperatures jump and the wall heat flux can be evaluated from

$$T_{\delta,v} - T_{\delta,L} = (T_{\delta,v} - T_w)/\left[1 + \left(\frac{h_{fg}\Omega}{k}\right)\delta\right] \tag{44}$$

$$q = k(T_{\delta,L} - T_w)/\delta. \tag{45}$$

All of the liquid properties appearing in the foregoing equations are to be evaluated at the reference temperature T^* given by equation (37), wherein T_δ corresponds to $T_{\delta,L}$.

An alternate, but approximate, formulation may be made by assuming that the expressions stemming from the Nusselt model can be applied locally. In essence, this ignores the history of the flow upstream of the point of interest. In other words, the similarity solution is assumed to apply locally. By taking the

† During the review process, an alternative model of the interfacial phenomena was brought to the attention of the authors. The alternative approach, which employs Grad's 13-moment molecular velocity distribution, is described in [22]. At this time, there is no clear-cut manner of assessing which of the models leads to heat transfer results that are closer to reality.

Nusselt expression for $\delta(x)$ and introducing the local thermal driving force $(T_{\delta,L} - T_w)$ there follows

$$\delta^4 = \frac{4\nu^2}{g}\left[\frac{c_p(T_{\delta,L} - T_w)}{Pr\, h_{fg}}\right]x \qquad (46)$$

Equations (44) and (45) remain as before, and the properties are to be evaluated at the reference temperature. Simultaneous solution of equations (46) and (44) yield δ and $T_{\delta,L}$, and with these, the heat flux is evaluated from equation (45).

As will be demonstrated in a later graphical presentation, the wall heat flux results calculated from the exact solution and from the approximate local-similarity solution are in very good agreement. This lends support to the application of the local-similarity concept to problems involving noncondensable gas and/or superheated vapor, in which cases similarity solutions are not possible in the presence of interfacial resistance.

Noncondensable gas and/or superheating

When applied to the general case involving noncondensables and/or superheating, the local-similarity concept leads to the following mathematical description of the problem: The similarity differential equations (3) and (18–20) continue to apply, but at a specific x location. All the boundary, continuity, and constraint conditions also continue to apply on the same basis, except for interfacial temperature continuity, equation (31), which is deleted. In its stead, one employs the temperature jump condition, equation (39). When the latter is rephrased in terms of the variables of the analysis, there is obtained

$$f(\eta_\delta) = [\Omega T_\infty x^{\frac{1}{2}}/3c\mu_w][\theta(\eta_\delta) - \Theta(0)] \qquad (47)$$

in which Ω is given by equation (42). Inasmuch as $T_{\delta,v}$, i.e. $\Theta(0)$, is unknown *a priori*, so also is Ω.

The explicit appearance of $x^{\frac{1}{2}}$ in equation (47) is a direct indicator of the non-similar nature of the problem. In order to proceed with the local-similarity solution, it is necessary to specify the x-location of interest. Once this has been done, the details of the numerical solution method are only slightly different from those for the similarity case. After solutions have been found, the local wall heat flux q is evaluated as before from equation (36) and then compared with q_{Nu} as given by equation (38). The reference temperature for the latter is specified by equation (37), with T_δ taken as $T_{\text{sat},\infty}$.

HEAT TRANSFER RESULTS

Noncondensable gas

The effect of the presence of a noncondensable gas on the local wall heat flux is displayed in Figs. 1–5. The first two figures pertain to the case where the bulk is saturated, that is $T_\infty = T_{\text{sat},\infty}$. The last three of these figures are for the situation in which the bulk is superheated. All the results to be discussed in this section correspond to the condition where interfacial resistance and thermal diffusion/diffusion thermo have been suppressed. These effects will be discussed later.

Attention is first directed to the results for the saturated mixture, Figs. 1 and 2. Each one of these figures is, in turn, subdivided into separate graphs, and each graph pertains to a specific value of $T_{\text{sat},\infty}$ in the range from 671·7°R (212°F) to 539·7°R (80°F). The corresponding range of the total pressure p is from approximately one atmosphere to 0·5 psi. In each graph, there are plotted results corresponding to bulk concentrations W_∞ of the noncondensable gas ranging from 0·001 to 0·1. The abscissa is the temperature difference between the saturated bulk and the wall.

Inspection of the figures reveals that the presence of a noncondensable gas has a decisive effect in reducing the condensation heat transfer. It is especially interesting to observe that reductions of more than 50 per cent are sustained for bulk mass fractions W_∞ as small as 0·5 per cent. With increasing values of W_∞, the heat flux decreases monotonically. At a fixed value of W_∞, the reduction in heat transfer (relative

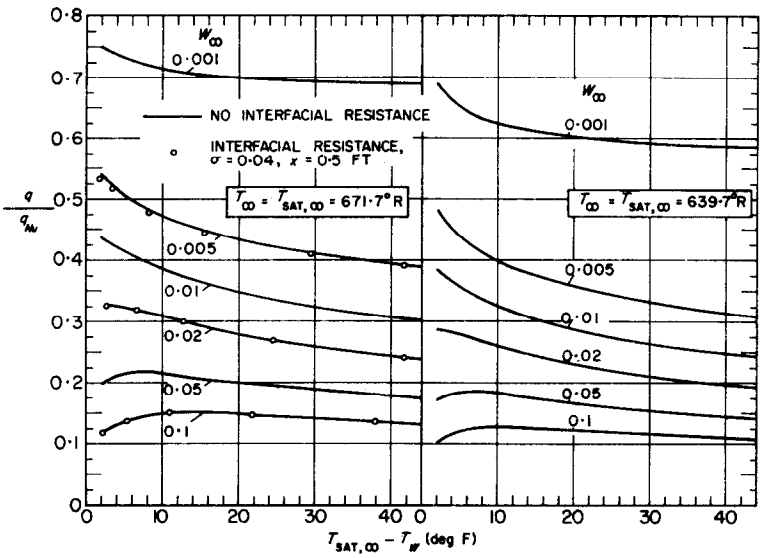

FIG. 1. Condensation heat transfer in the presence of a noncondensable gas, saturated bulk, $T_{sat,\infty} = 671{\cdot}7°R$ and $639{\cdot}7°R$.

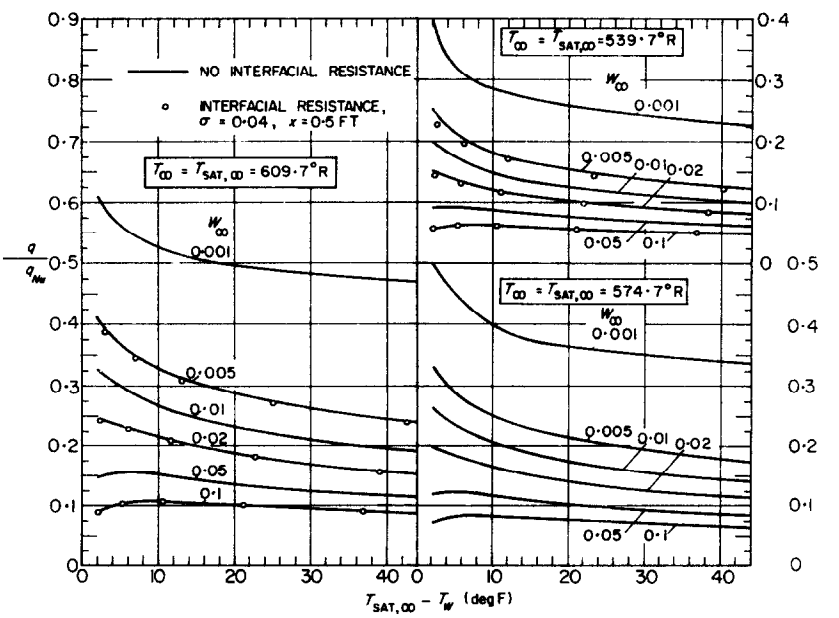

FIG. 2. Condensation heat transfer in the presence of a noncondensable gas, saturated bulk, $T_{sat,\infty} = 609{\cdot}7°R$, $574{\cdot}7°R$, and $539{\cdot}7°R$.

to q_{Nu}) is larger as the bulk-to-wall temperature difference increases, except at small temperature differences and larger W_∞. Furthermore, by making comparisons from graph-to-graph, it is seen that the effect of the noncondensable gas is strongly accentuated as the bulk saturation temperature (i.e. system pressure level) decreases.

The fact that such large reductions in heat transfer are brought about by such small bulk concentrations of noncondensable gas can be made plausible on the following physical grounds: The vapor that is to be condensed is carried from the bulk to the interface by convective flow, which also carries with it the noncondensable gas. However, since the interface is impermeable to the noncondensable gas, it must be removed from the interface at the same rate at which it arrives. This removal is accomplished by a diffusive flow back into the bulk. Inasmuch as the magnitude of the diffusive flow depends on the magnitude of the concentration gradient, it is evident that the interfacial concentration of the noncondensable gas must build up to a level sufficient for the balance between the convective inflow and diffusive backflow.

The buildup of the noncondensable gas at the interface causes a corresponding reduction in the partial pressure of the vapor at the interface. In turn, this reduces the saturation temperature at which the condensation takes place. The net effect is to lower the effective thermal driving force $(T_\delta - T_w)$ thereby reducing the heat transfer.

All of the trends that were enumerated in connection with Figs. 1 and 2 can be explained in light of the foregoing arguments, except for the droping off of the curves at small $(T_{sat,\infty} - T_w)$ and larger W_∞. This latter behavior occurs because T_δ approaches closely to T_w for small, non-zero values of $(T_{sat,\infty} - T_w)$.

Consideration will now be given to the effect of noncondensable gases for the case of superheated vapor, Figs. 3–5. Each one of these figures pertains to a specific value of W_∞, respectively 0·005, 0·02, and 0·1. Furthermore,

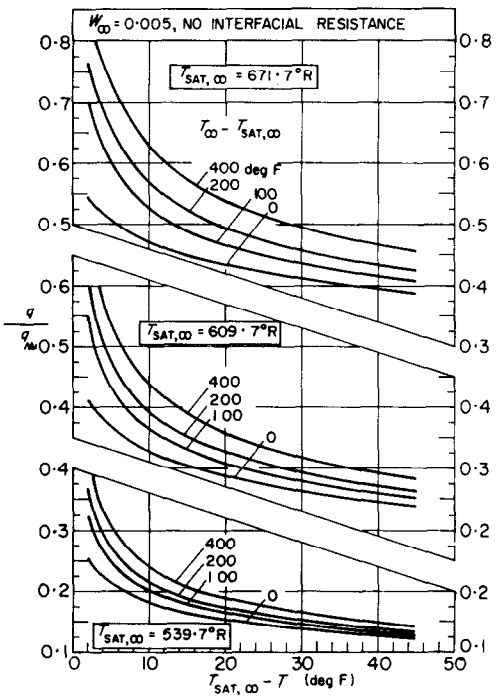

FIG. 3. Condensation heat transfer in the presence of a noncondensable gas, superheated bulk, W_∞ = 0·005.

each figure is subdivided into 3 grids. Each grid corresponds to a given value of $T_{sat,\infty}$. The various curves that are plotted within each grid are parameterized by the degree of superheating, $(T_\infty - T_{sat,\infty})$. The ordinate is the ratio of the heat flux q to the Nusselt value q_{Nu} the latter corresponding to $(T_{sat,\infty} - T_w)$ as thermal driving force. The abscissa remains as before.

Careful inspection of these figures reveals that all of the qualitative effects stemming from the presence of the noncondensable gas are identical to those already enumerated for the case of saturated mixtures. The plausibility arguments previously advanced continue to apply. The reduction in heat transfer due to the noncondensable gas is somewhat lessened owing to the opposite effect of superheating. This aspect will be brought out more strongly in the next section.

As a final note, it is well to reiterate that the large reductions in heat transfer that have

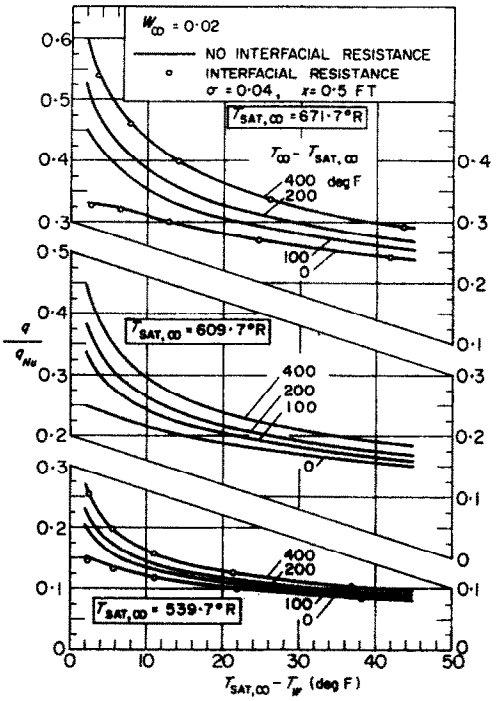

FIG. 4. Condensation heat transfer in the presence of a non-condensable gas, superheated bulk, $W_\infty = 0{\cdot}02$.

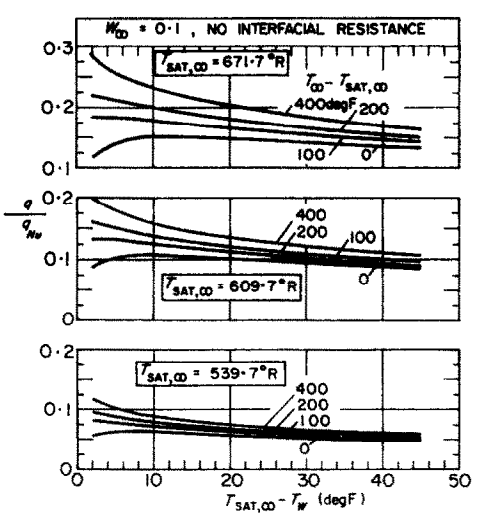

FIG. 5. Condensation heat transfer in the presence of a non-condensable gas, superheated bulk, $W_\infty = 0{\cdot}1$.

thus far been discussed in connection with Figs. 1–5 are due entirely to the diffusional resistance of the mixture.

Superheating

Consideration is first given to the effect of superheating a pure vapor. To this end, Fig. 6

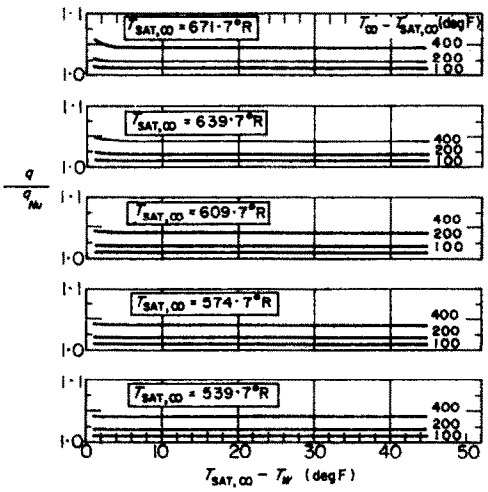

FIG. 6. Condensation heat transfer for pure superheated vapor.

has been prepared. The figure contains five grids, each for a different value of $T_{sat,\infty}$. In each grid, results are shown for superheats of 100 degF, 200 degF, and 400 degF. On the ordinate, q is normalized by q_{Nu}, the latter corresponding to zero superheat. Thus, the deviation of the curves from unity is a direct measure of the increase in the wall heat transfer due to superheating.

The figure shows that superheating brings about only a slight increase in the heat transfer during the condensation of a pure vapor. Furthermore, for a given degree of superheating, q/q_{Nu} is almost independent of $T_{sat,\infty}$ and of $(T_{sat,\infty} - T_w)$. However, when the latter takes on very small values, it is expected that q/q_{Nu} will become large, owing to the diminution of the condensation rate (i.e. $q_{Nu} \to 0$). Such a trend is suggested by the uppermost curves in the top two grids of the figure.

It is interesting to compare the present results with those of Sparrow and Eckert [4], who neglected both free convection and variable properties in the superheated vapor. For example, for the case of 400 degF superheating and $T_{sat,\infty} = 671{\cdot}7°F$, the latter investigators predict $q/q_{Nu} = 1{\cdot}045$, which compares favorably with the present value of 1·047. This suggests that, at least for the case of a pure vapor, the role of free convection is insignificant.

Attention may next be directed to the effect of superheating in the case when a noncondensable gas is present, and for this, one returns to Figs. 3–5. The structure of these figures has already been explained. Study of the figures indicates that for given values $T_{sat,\infty}$, $(T_{sat,\infty} - T_w)$, and W_∞, the percentage increase in heat transfer due to superheating (i.e. relative to zero superheating) is substantially larger than in the case of a pure vapor (Fig. 6). This is especially true for high $T_{sat,\infty}$, small $(T_{sat,\infty} - T_w)$, and low W_∞. Indeed, for these conditions, the absolute increase in q due to superheating far exceeds that for the pure vapor.

Thus, the present results show that while superheating is very nearly a negligible effect in the case of pure vapors, it may be an important factor during the condensation of vapors that contain a noncondensable gas.

Interfacial resistance

It is revealing to consider first the effects of interfacial resistance on the condensation heat transfer of a pure saturated vapor. This information is shown in Fig. 7. Owing to the fact that the presence of interfacial resistance precludes similar solutions, it is necessary to specify the x-location for which results are desired. The left-hand portion of Fig. 7 corresponds to $x = 0{\cdot}5$ ft, while the right-hand portion corresponds to $x = 3$ ft.

The figure is subdivided into several grids,

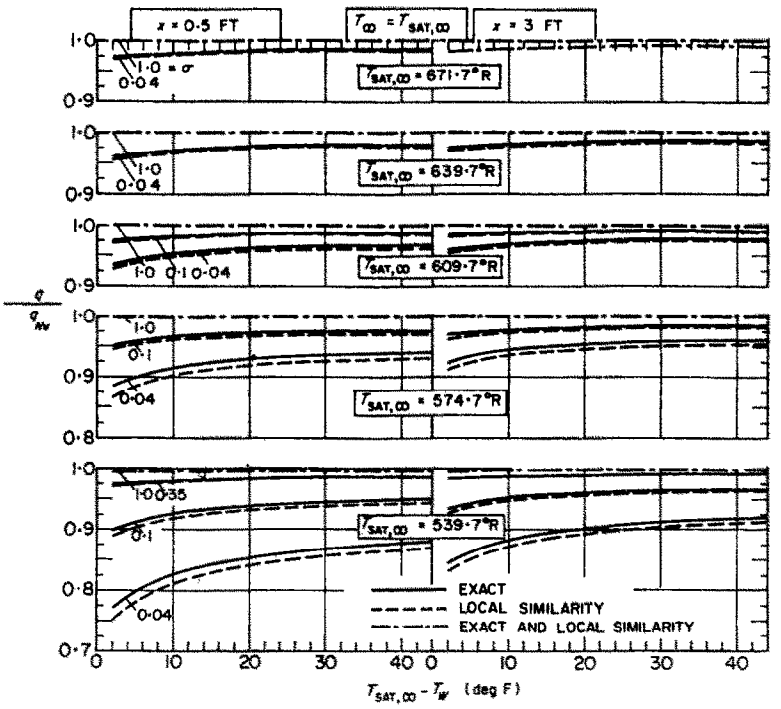

FIG. 7. Effect of interfacial resistance on the condensation heat transfer of pure saturated vapor.

each of which contains curves for a specific value of $T_{sat,\infty}$. The solid lines represent the exact solution, while the dashed lines are for the local-similarity solution. When the two solutions are essentially coincident, then a dot-dashed line is used. The curve parameter σ is the condensation coefficient. Inasmuch as q_{Nu} is based on $(T_{sat,\infty} - T_w)$ as thermal driving force, the deviation of the curves from unity is a direct measure of the role of interfacial resistance.

From an inspection of the figure, it is seen that the effect of the interfacial resistance is most in evidence at very small values of σ and at low $T_{sat,\infty}$ and $(T_{sat,\infty} - T_w)$. On the other hand, the interfacial resistance is fully negligible at the higher $T_{sat,\infty}$ (higher pressures), no matter what the value of σ. Furthermore, if σ is 0·35 or greater, then the interfacial resistance plays no role, regardless of the values of $T_{sat,\infty}$ or $(T_{sat,\infty} - T_w)$. All of the aforementioned trends can also be deduced by physical reasoning with the aid of equation (39).

It is appropriate, at this point, to consider the available information for σ. Values for σ of approximately 0·04 have been given by several investigators [20, 21]. However, the very recent results of Nabavian [21] suggest that a more probable range for σ is 0·35–1·0. Even more recently, Mills [22] performed a condensation experiment with pure saturated steam and showed that σ is essentially unity. In addition, it is demonstrated in [22] that the experiments of Hickman are consistent with a σ of unity. If one adopts the σ values from these most recent studies, then it would appear that the effect of interfacial resistance can be neglected.

A comparison of the solid and the dashed curves appearing in Fig. 7 shows that the differences between the exact solution and the local-similarity solution are, for all practical purposes, negligible. This finding lends support for the use of the latter model for the case wherein noncondensables and/or superheating are present.

As a final comment in connection with Fig. 7, it may be observed that the effect of the interfacial resistance decreases with increasing distance from the leading edge. This is readily explained by noting that the condensation rate $\dot{m}$ decreases with increasing x, and in accordance with equation (39), the temperature jump decreases correspondingly.

A presentation similar in form to Fig. 7, but for the case of a pure vapor with 400 degF superheat, is presented in Fig. 8. The results displayed in the figure are based on the local-similarity concept, inasmuch as an exact solution cannot be attained. The trends that are in evidence in this figure are identical to those discussed in connection with Fig. 7 and need not be repeated.

For cases in which there is a noncondensable gas and/or superheating, the effect of the interfacial resistance is displayed in Figs. 1, 2, and 4. Inasmuch as the q/q_{Nu} values corresponding to the presence of interfacial resistance were found to fall very close to those without this effect, the former are plotted as discrete points so as to maintain their separate identity. In order to exaggerate the role of interfacial resistance, points corresponding to $\sigma = 0{\cdot}04$ are shown. If results for $\sigma = 1{\cdot}0$ had been plotted, then the points would have fallen squarely on the solid curves. It is evident from an inspection of these figures that the interfacial resistance plays a negligible role in the condensation of steam when air is present as a noncondensable gas.

Thermal diffusion and diffusion thermo

Solutions including thermal diffusion and diffusion thermo were carried out for cases corresponding to the extreme values of the independent parameters; interfacial resistance was suppressed. The heat transfer results stemming from these solutions are plotted as discrete points in Fig. 9 in order to preserve their identity. The solid curves represent results wherein thermal diffusion and diffusion thermo are absent. It is seen from the figure that the points are essentially coincident with the curves,

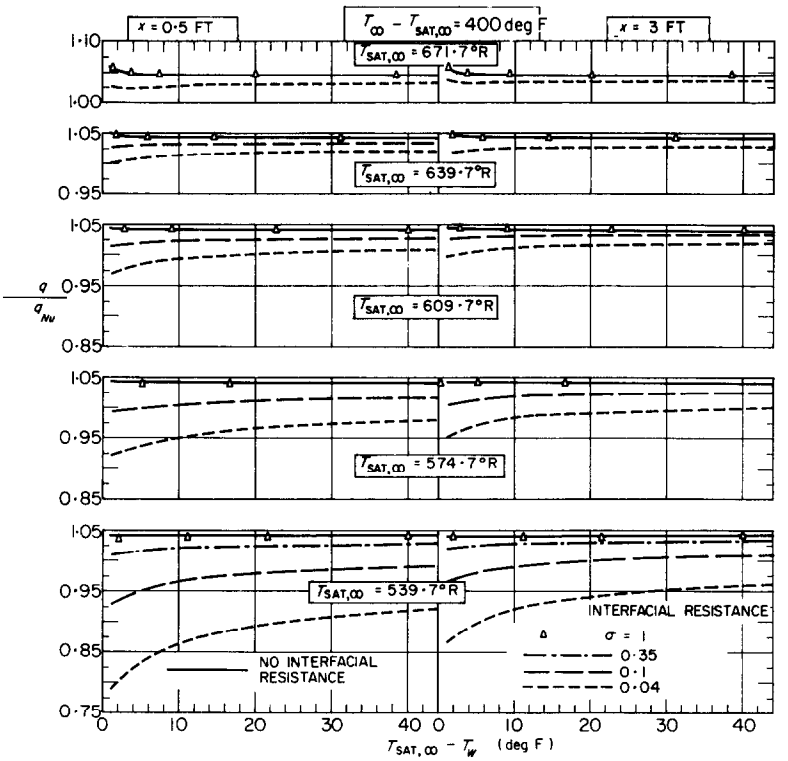

FIG. 8. Effect of interfacial resistance on the condensation heat transfer of pure superheated vapor.

thereby indicating that the thermal diffusional phenomena are of no significance in this situation.

Comparisons with others

Within the knowledge of the authors, the only systematic experiments on the condensation of steam with air as a noncondensable were performed by Othmer [23]. The experimental apparatus consisted of a cooled horizontal cylinder situated in an enclosure containing a saturated mixture of steam and air at essentially one atmosphere. Measurements were made of the overall rate of heat transfer Q for a range of surface temperatures T_w.

Inasmuch as the physical system of the experiment differs from that investigated here, the only reasonable comparison is of Q/Q_0 values, where Q_0 is the overall condensation rate in the absence of noncondensables.† Unfortunately, the experimental determinations of Q and Q_0 were, in general, not performed at the same value of $(T_{sat,\infty} - T_w)$, and after appraisal of the data, it was decided that interpolation would not lead to reliable results. Only at a temperature difference of 10 degF were the Q and Q_0 both available. The corresponding experimental points are shown in Fig. 10. Also shown as solid lines are the Q/Q_{Nu} predictions of the present analysis. The level of agreement is about as good as can be hoped for in view of the difficulty encountered in performing such experiments and of the differences in the physical system investigated.

There are also shown in the figure dashed lines that represent the predictions of the

† For the analytical results, $Q_0 = Q_{Nu}$.

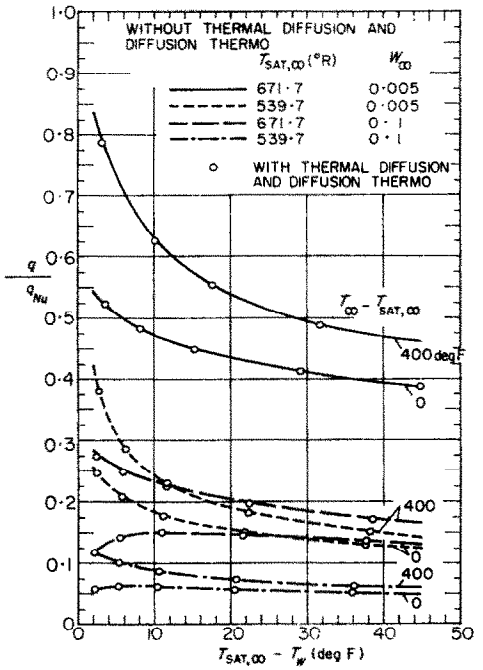

FIG. 9. Effect of thermal diffusion and diffusion thermo on condensation heat transfer.

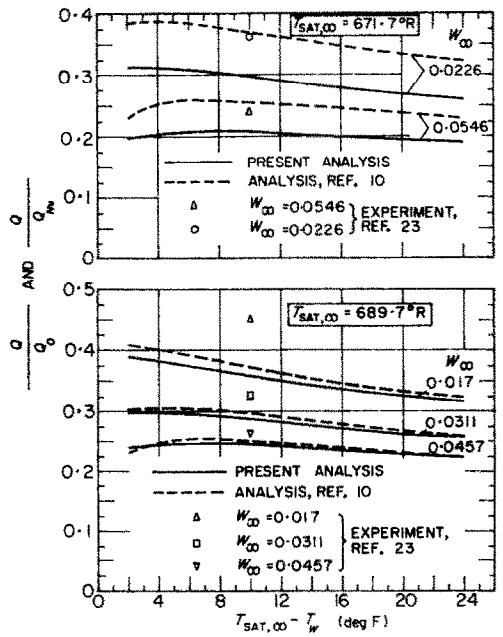

FIG. 10. Comparison of analytical and experimental heat-transfer results.

constant-property analysis of Sparrow and Lin [10]. At first glance, it appears that the constant-property results are in better agreement with the data than are the present results. However, this is illusory, since the property values used in parameterizing the constant-property analysis are somewhat different from those appropriate to the specific situation under consideration, especially in the case $T_{sat,\infty} = 671{\cdot}7°R$. This difficulty arises because the constant-property analysis cannot be readily tailored to fit any arbitrary case of interest. However, it can be reasoned that if the appropriate property values are employed, the predictions of the constant-property analysis are shifted downward toward those of the analysis.

REPRESENTATIVE TEMPERATURE PROFILES

Some insight into the role of the various transport processes can be obtained by inspection of the boundary layer temperature profile. To this end, two representative temperature profiles are displayed in Fig. 11. Both profiles correspond to saturated vapor at $T_{sat,\infty} = 539{\cdot}7°R$ and $W_\infty = 0{\cdot}02$. The temperature difference between the fluid bulk and the wall is 10 degF. The uppermost temperature profile is for the case $\sigma = 0{\cdot}04$, while the lower profile is for $\sigma = 1{\cdot}0$.

In preparing the figure, it was decided that a better physical feel would be obtained if dimensional quantities, rather than dimensionless quantities, were employed as ordinate and abscissa variables. Inasmuch as the thickness of the condensate layer ($\sim 0{\cdot}001$ in.) is three orders of magnitude less than the thickness of the vapor-gas boundary layer, a broken abscissa scale had to be employed.

Upon considering the figure, it is seen that the largest part of the overall temperature drop between the bulk and the wall occurs within the vapor–gas boundary layer. This underscores the decisive role of the diffusional resistance in the vapor–gas boundary layer. The interfacial resistance, although exaggerated by a small value of σ ($=0{\cdot}04$) and a low value of $T_{sat,\infty}$,

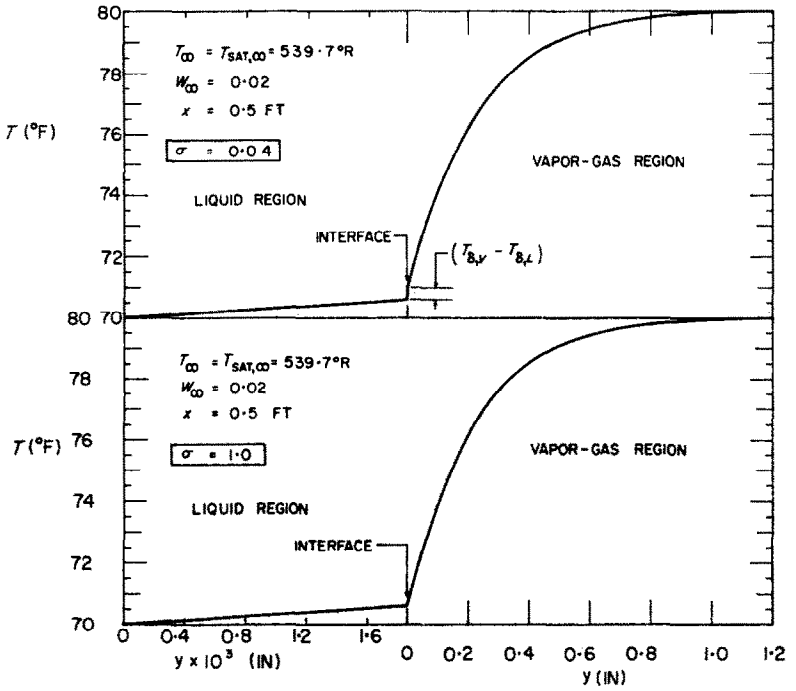

FIG. 11. Representative temperature profiles.

gives rise to a temperature jump that is much smaller than the temperature difference due to the diffusional resistance. It is also interesting to note that $(T_{\delta,L} - T_w)$ is almost identical in the two cases, in spite of the fact that a temperature jump is present in one and not in the other.

Representative mass fraction profiles have been presented in [13], but must be omitted here owing to space limitations.

REFERENCES

1. W. NUSSELT, The surface condensation of water vapor (in German), *Z. Ver. Dt. Ing.* **60**, 541–546, 596–575 (1916).
2. D. J. WILHELM, Condensation of metal vapors: Mercury and the kinetic theory of condensation, Argonne National Laboratory Report 6948 (1964).
3. W. STENDER, Heat transmission during condensation of superheated steam (in German). *Z. Ver. Dt. Ing.* **69**, 905–909 (1925).
4. E. M. SPARROW and E. R. G. ECKERT, Effects of superheated vapor and non-condensable gases on laminar film condensation, *A.I.Ch.E. Jl* **7**, 473–477 (1961).
5. R. S. SILVER, Heat transfer coefficients in surface condensers, *Engineering, Lond.* **161**, 505–507 (1946).
6. R. S. SILVER and H. C. SIMPSON, The condensation of superheated steam, Proceedings of a Conference held at the National Engineering Laboratory, East Kilbride, Glasgow, 14–15 March 1961. Her Majesty's Stationery Office, Edinburgh (1962).
7. S. P. SUKHATME and W. M. ROHSENOW, Heat transfer during film condensation of a liquid metal vapor, ASME paper 65-HT-29, to be published in *J. Heat Transfer*.
8. E. F. M. VAN DER HELD, Der Einfluss der Anwesenheit von Luft auf die Kondensation von Wasserdampf, *Physica's Grav.* **1**, 1153–1160 (1934).
9. A. P. COLBURN and T. B. DREW, The condensation of mixed vapors, *Trans. Am. Inst. Chem. Engrs* **33**, 197–208 (1937).
10. E. M. SPARROW and S. H. LIN, Condensation heat transfer in the presence of a noncondensable gas, *J. Heat Transfer* **C86**, 430–436 (1964).
11. W. M. ROHSENOW and H. Y. CHOI, *Heat, Mass, and Momentum Transfer*, Prentice-Hall, Englewood Cliffs, N.J. (1961).
12. J. C. Y. KOH, E. M. SPARROW and J. P. HARTNETT, The two-phase boundary layer in laminar film condensation, *Int. J. Heat Mass Transfer* **2**, 69–82 (1961).
13. W. J. MINKOWYCZ, Laminar film condensation of water vapor on an isothermal vertical surface, Ph.D. Thesis, Department of Mechanical Engineering, University of Minnesota, Minneapolis, Minnesota (1965).
14. E. R. G. ECKERT and R. M. DRAKE, JR., *Heat and*

Mass Transfer, 2nd edn. McGraw-Hill, New York (1959).
15. E. A. MASON and L. MONCHIK, Survey of the equation of state and transport properties of moist gases, 1963 International Symposium on Humidity and Moisture, National Bureau of Standards, Washington, D.C. (1963).
16. J. HILSENRATH, *Tables of Thermodynamic and Transport Properties of Gases*. Pergamon Press, New York (1960), also National Bureau of Standards Circular No. 564 (1955).
17. J. H. KEENAN and F. G. KEYES, *Thermodynamic Properties of Steam*. John Wiley, New York (1949).
18. R. W. SCHRAGE, *A Theoretical Study of Interphase Mass Transfer*. Columbia University Press, New York (1953).
19. G. BALEKJIAN and E. T. KATZ, Heat transfer from superheated vapors to a horizontal tube, *A.I.Ch.E. Jl* **4**, 43–48 (1958).
20. B. PAUL, Compilation of evaporation coefficients, *ARS Jl* **32**, 1321–1328 (1962).
21. K. NABAVIAN, Condensation coefficient of water, Ph.D. Thesis, University of California, Berkeley (1962).
22. A. F. MILLS, The condensation of steam at low pressures, Technical Report on NSF GP-2520, Series No. 6, Issue No. 39. Space Sciences Laboratory, University of California, Berkeley, November (1965).
23. D. F. OTHMER, The condensation of steam, *Ind. Engng Chem.* **21**, 577–583 (1929).
24. S. S. KUTATELADZE, *Fundamentals of Heat Transfer*, pp. 298–326. Edward Arnold, London (1963).

Zusammenfassung—Eine eingehende analytische Untersuchung der laminaren Filmkondensation wird vorgelegt. Untersucht wird eine isotherme senkrechte Platte mit Wasserdampf als kondensierendes Medium und Luft als Inertgas. Neben dem Inertgas schliesst das analytische Modell den Übergangswiderstand, die Überhitzung, die freie Konvektion und die Diffusion infolge von Temperatur- und Konzentrationsgradienten und die veränderlichen Eigenschaften sowohl im Flüssigkeits- als auch im Gas-Dampf-Bereich mit ein. Ergebnisse für den Wärmeübergang werden für einen weiten Umfang von Parametern erhalten, nämlich die Massenkonzentration des Inertgases, die Höhe des Systemdruckes, die Temperaturdifferenz zwischen Kühlfläche une Dampfraum und den Grad der Überhitzung. Es wird gezeigt, dass eine geringe Massenkonzentration an Inertgas eine entsheidende Wirkung auf den Wärmeübergang haben kann. Zum Beispiel wird für einen Massenanteil von 0,5 Prozent an Luft der Wärmeübergang um 50 Prozent oder mehr vermindert. Der Einfluss des Inertgases tritt bei niedrigen Drucken noch stärker hervor. Es zeigt sich, dass die zuvor erwähnte Herabsetzung des Wärmeübergangs vollkommen vom Diffusionswiderstand der Gas-Dampf-Grenzschicht verursacht wird. Der Übergangswiderstand ist, wie gezeigt wird, ein Effekt 2. Ordnung. Ähnliche Ergebnisse rühren vom Thermodiffusions- und vom Diffusionsthermoeffekt her. Der Einfluss der Überhitzung, der sehr gering für einen reinen Dampf ist, wird bei Vorhandense in eines nichtkondensierbaren Gases sehr viel bedeutsamer. Eine Regel für die Bezugstemperatur wird abgeleitet, um das Nusselt-Modell auf Bedingungen mit veränderlichen Eigenschaften zu erweitern.

Аннотация—Дается обширное аналитическое исследование ламинарной пленки, образующейся при конденсации. Рассматривается случай изотермической вертикальной пластины, обтекаемой конденсирующимся паром при наличии воздуха в качестве неконденсирующего газа. Кроме неконденсирующего газа аналитическая модель включает также сопротивление на границе раздела фаз, перегрев и свободную конвекцию, обусловленную градиентами температуры и концентрации, массовую и термическую диффузию, а также переменные свойства как в жидкости, так и в газопаровой смеси. Данные по теплообмену получены для широкого диапазона параметров, включающих массовую концентрацию неконденсированного газа, давление в системе, разность температур между средой и стенкой и степень перегрева. Показывается, что небольшие массовые концентрации неконденсирующегося газа могут значительно влиять на скорость теплообмена. Например, для массовой концентрации воздуха (0,5%) наблюдается уменьшение теплообмена до 50% и более. Влияние неконденсирующего газа проявляется при низких давлениях. Показано, что указанное выше уменьшение теплообмена происходит полностью за счёт диффузионного сопротивления слоя на границе газ-пар. Сопротивление на границе раздела фаз имеет второстепенное значение. Аналогичный подход применяется к термической диффузии и термодиффузионому сопротивлению. Влияние перегрева, которое очень мало в случае чистого пара, становится значительным при наличии неконденсирующегося газа. Для применения числа Нуссельта к условиям переменных свойств, выведено правило нахождения определяющей температуры.